PROCEEDINGS OF SCIENCE

Review of p_t fluctuations and correlations

Duncan J. Prindle* **and Thomas A. Trainor (STAR Collaboration)**
University of Washington
E-mail: prindle@npl.washington.edu,
trainor@hausdorf.npl.washington.edu

We describe the origins of $\langle p_t \rangle$ fluctuations in terms of local p_t spectrum shape changes on (η, ϕ). We review fluctuation measure design and $\langle p_t \rangle$ fluctuation measurements at the SPS and RHIC. We show that p_t angular autocorrelations derived from the scale dependence of $\langle p_t \rangle$ fluctuations reveal a complex parton scattering and dissipation process in RHIC heavy ion collisions. From p_t correlation structure in heavy ion collisions we observe for the first time temperature/velocity structure resulting from copious low-Q^2 parton scattering. We also observe novel structure which could result from collective bulk-medium recoil in response to parton stopping. The energy dependence of $\langle p_t \rangle$ fluctuations is strong and consistent with QCD energy trends.

Correlations and Fluctuations in Relativistic Nuclear Collisions
July 7-9 2006
Florence, Italy

*Speaker.

PoS(CFRNC2006)007

1. Introduction

From the inception of the relativistic heavy ion program at the Bevalac study of nuclear matter at large energy density and the possibility of a transformation to color-deconfined or QCD matter have been the central goals. Au-Au collisions at RHIC may generate a color-deconfined medium (quark-gluon plasma or QGP) [1]. By analogy with the thermodynamics of ordinary matter critical fluctuations have been viewed as a means to demonstrate transitions across the QCD phase boundary. In particular, critical fluctuations of $\langle p_t \rangle$ or event-wise mean p_t as an analog to temperature have been sought. In RHIC data we indeed observe excess fluctuations. A measurement of $\langle p_t \rangle$ fluctuations in Au-Au collisions at 130 GeV first revealed large-amplitude fluctuations compared to independent-particle p_t production [2]. Subsequent measurements have confirmed and elaborated those observations [3, 4, 5, 6].

$\langle p_t \rangle$ fluctuations observed at RHIC are not critical fluctuations in the thermodynamic sense. Excess fluctuations have been traced, through equivalent p_t angular correlations, to hadron fragments from copious low-Q^2 partons (minijets). Some theories describe abundant low-Q^2 parton (gluon) production in the early stages of high-energy nuclear collisions and rapid parton thermalization as the production mechanisms for the colored medium [7, 8, 9]. Given the demonstrated connection between partons and $\langle p_t \rangle$ fluctuations, excess $\langle p_t \rangle$ fluctuations may thus help to reveal both the production mechanism and the properties of the QCD medium. From fluctuation and correlation analysis we find strong evidence for minijets which are not fully thermalized. Final-state minijet structure at full RHIC energy may actually obscure any QCD critical fluctuations. Following the strategy of Penzias and Wilson when faced with a similar dilemma in the study of microwave transmission, we conclude that if we can't get rid of the noise (minijets) we should study the noise. In so doing we find ourselves rediscovering QCD "from the bottom up."

In this paper we describe the event-wise angular distributions of transverse momentum p_t produced in relativistic nuclear collisions at RHIC. We present the algebraic relation between mean-p_t fluctuations and p_t angular correlations. We compare angular autocorrelations on (η, ϕ) to conventional leading-particle techniques for parton fragment analysis. We present experimental evidence from mean-p_t fluctuations and corresponding p_t angular autocorrelations for local temperature/velocity structure in A-A collisions. We suggest that such structure can be interpreted in terms of parton fragmentation in the A-A medium and *recoil response* of the QCD medium to parton stopping. Finally, we review the energy dependence of mean-p_t fluctuations from SPS to RHIC and its implications.

2. What are $\langle p_t \rangle$ fluctuations?

$\langle p_t \rangle$ fluctuations were expected to reflect variations of global event temperature T assuming that each collision achieved a thermalized final state, with a different "temperature" for each event. We have been forced by RHIC data to reconsider that picture, to develop a model-independent fluctuation analysis which can accommodate a variety of unanticipated phenomena. More generally, $\langle p_t \rangle$ fluctuations result from event-wise changes in the (η, ϕ) dependence of the shape of the single-particle p_t spectrum. The technical challenge is representing those changes with minimal distortion in a form which can be interpreted physically.

Each hadron p_t samples a *local parent* spectrum shape depending on the sample location, as shown by a cartoon of the sampling process in Fig. 1 (first panel). Variation of the local parent shape may be arbitrarily structured on (η,ϕ). The angular acceptance is divided into bins $(\delta\eta,\delta\phi)$, which may each contain one or many particles depending on bin size. The total p_t in a bin is a sample from the local parent spectrum for that angular bin and event. The event-wise local-parent shape can be characterized schematically by parameter $\beta(\eta,\phi)$. β can be interpreted loosely as inverse slope $1/T$ or relative speed v/c, a property of the local pre-hadronic medium (the particle source). Variation of either or both parameters relative to an ensemble mean results in $\langle p_t\rangle$ fluctuations. Possible spectrum shape variations are sketched in the second panel.

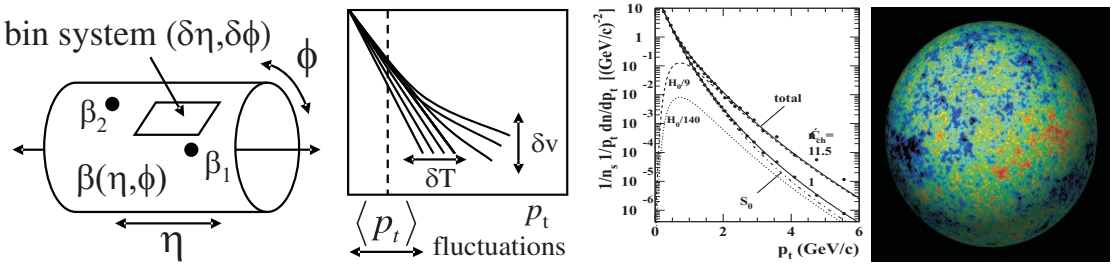

Figure 1: Sampling p_t spectra and shape parameter β on a binned angular acceptance; possible sources of $\langle p_t\rangle$ fluctuations; measure p_t spectra for two multiplicity classes from 200 GeV p-p collisions; WMAP CMB microwave power distribution on the unit sphere.

In Fig. 1 (third panel) we show measured p_t spectra for p-p collisions from two multiplicity classes [10], revealing a real manifestation of the sketch in the second panel. The p_t spectrum can be separated into soft component S_0 and hard component H_0, because the H_0 abundance relative to S_0 is simply proportional to the event multiplicity. The hard component occurs as a minijet in about 1% of NSD p-p collisions and is localized on (eta,phi) differently in each event. In Au-Au collisions at RHIC multiple minijet structures are distributed on (η,ϕ) in each event and can be interpreted as local variations of the velocity/temperature of the medium [2, 11].

A similar situation emerges in studies of the cosmic microwave background (CMB), as shown in Fig. 1 (fourth panel) [12]. The microwave power density (local spectrum integral rather than mean) represents the temperature distribution (inverse β) on the unit sphere. The $\beta(\theta,\phi)$ structure for that single event is directly observable due to the large photon flux. In contrast, for a single Au-Au collision the parent spectrum is sparsely sampled by ~ 1000 final-state hadrons, and parent properties are not accessible on an event-wise basis. However, for an ensemble of many heavy ion collisions the two systems are comparable at the level of autocorrelations/power spectra.

Interpretation of $\langle p_t\rangle$ fluctuations is achieved by two complementary routes: 1) construct number correlations on (p_t,p_t) or (y_t,y_t) which include the two-particle parton fragment distribution [11, 13, 14]; 2) invert the *scale or bin-size dependence* of $\langle p_t\rangle$ fluctuations to obtain p_t angular autocorrelations on $(\eta_\Delta,\phi_\Delta)$ [4, 15]. Those methods, applied to Au-Au collisions at RHIC, have revealed partially-dissipated minijets or equivalently the structure of the event-wise $\beta(\eta,\phi)$ distribution on the prehadronic medium.

3. $\langle p_t \rangle$ fluctuation measures

Initial fluctuation measures assumed that a few global event variables could fully characterize thermalized heavy ion collisions. Comparing the variance of a global variable to a statistical reference should then extract all available information. $\langle p_t \rangle$ was intended to estimate a global temperature. It should fluctuate with a 'statistical' component and a component reflecting collision dynamics in some way to be determined. Comparing $\sigma^2_{\langle p_t \rangle}$ to $\sigma^2_{\hat{p}_t}/\bar{n}$ as a central-limit reference (independent p_t samples from a fixed parent spectrum) should then constitute a complete fluctuation measurement and reveal 'dynamical' collision details.

Several fluctuation measures defined at the SPS and RHIC were based on those expectations, e.g., $\sigma^2_{p_t,dynamical} \equiv \sigma_{\langle p_t \rangle} - \sigma^2_{\hat{p}_t}/\bar{n}$ [16] and $F_{p_t} \equiv \sigma_{\langle p_t \rangle,data}/\sigma_{\langle p_t \rangle,mixed} - 1$, with $\sigma_{\langle p_t \rangle,mixed} \sim \sigma^2_{\hat{p}_t}/\bar{n}$ [3, 17]. Because $\langle p_t \rangle = p_t/n$ is a ratio of random variables its variance becomes anomalously large for small $\bar{n}$, an example of measure bias. Both the above measures respond to n fluctuations as well as true p_t fluctuations and are dominated by a term proportional to $\sigma^2_n/\bar{n}^2 \sim 1/\bar{n}$ for small $\bar{n}$. A variant of $\sigma^2_{p_t,dynamical}$, $\langle \delta p_{ti} \cdot \delta p_{tj} \rangle = \overline{\left\{ \frac{\sum_{i \neq j} (p_{ti} - \hat{p}_t)(p_{tj} - \hat{p}_t)}{n(n-1)} \right\}}$ [5], substantially reduces bias, but at the expense of playing a role intermediate between fluctuation and correlation measurement which makes its interpretation difficult. Further adding to confusion are approximate relations among fluctuation measures which may be valid in a large-n limit but fail for small multiplicities. Attempts to 'simplify' the statistical measure landscape with such approximations have impeded progress in fluctuation/correlation analysis.

$\Phi_{p_t} \equiv \sqrt{\overline{(p_t - n\hat{p}_t)^2}/\bar{n}} - \sqrt{\sigma^2_{\hat{p}_t}}$ tests invariance of $\langle p_t \rangle$ fluctuations under superposition of independent systems [18], e.g., p-p linear superposition compared to A-A collisions [2, 4, 20]. A closely-related measure is based on Pearson's normalized covariance [21] $r_{ab} \equiv \frac{\sigma^2_{ab}}{\sqrt{\sigma^2_a \sigma^2_b}} \rightarrow \frac{\overline{(p_t - n\hat{p}_t)_a (p_t - n\hat{p}_t)_b}}{\sigma^2_{\hat{p}_t} \sqrt{\bar{n}_a \bar{n}_b}}$ which has the same property. We drop $\sigma^2_{\hat{p}_t}$ from the denominator to be consistent with other measures (discussed below), take $a = b$ and obtain $\Delta\sigma^2_{p_t:n} \equiv \overline{(p_t - n\hat{p}_t)^2}/\bar{n} - \sigma^2_{\hat{p}_t}$, a comparison between a normalized variance and its central-limit (CLT) reference [2, 22]. $\Delta\sigma^2_{p_t:n}$ is a variance difference whereas Φ_{p_t} is a difference between r.m.s. terms. In general, variances and covariances obey a linear algebra, and $\Delta\sigma^2_{p_t:n}$ is simply related to two-particle correlations (*cf.* Sec. 5).

Σ_{p_t} was motivated by a specific model of global temperature fluctuations in thermalized events. There are two versions: $\Sigma_{p_t} \equiv \sqrt{\Delta\sigma^2_{p_t:n}/\bar{n}\hat{p}_t^2}$ [24] and $\Sigma'_{p_t} \equiv \sqrt{\langle \delta p_{ti} \cdot \delta p_{tj} \rangle}/\hat{p}_t^2$ [5]. If the hypothesis of global thermalization underlying these definitions is not valid the meaning of either Σ_{p_t} is not clear. We find plentiful evidence that global thermalization is not satisfied in RHIC collisions. We return to the interpretation of Σ_{p_t} in Sec. 10 on the energy dependence of $\langle p_t \rangle$ fluctuations.

Can we isolate a "best" fluctuation measure for a particular application? Yes, if sufficient constraints are applied to design. The relation between correlations and fluctuations must be understood. The algebra of random variables, different from ordinary variables, must be respected. A carefully-designed statistical reference must be incorporated, as well as the capacity to test a linear-superposition hypothesis. Unambiguous separation and identification of different physical mechanisms is the ultimate goal. Given those constraints an optimum fluctuation measure for each application can be defined.

4. $\langle p_t \rangle$ fluctuation measurements

The first $\langle p_t \rangle$ fluctuation measurement, made by NA49 at the SPS for central Pb-Pb collisions at 17.3 GeV, is shown in Fig. 2 (first panel) [26]. A frequency histogram on $M(p_t) = \langle p_t \rangle$ (points) is compared to a mixed-pair reference (histogram). A quantitative comparison between data and reference was made with Φ_{p_t} [18]. No significant non-statistical fluctuations were observed in the rapidity acceptance y_π =[4,5.5]. NA49 has subsequently obtained nonzero results at 17.3 GeV for more peripheral Pb-Pb collisions [27].

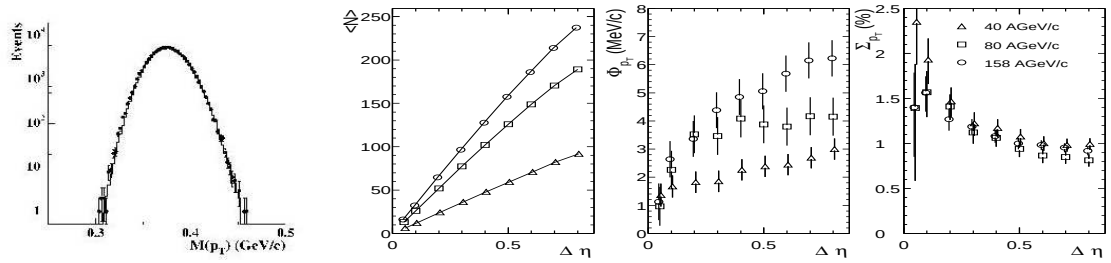

Figure 2: Frequency distribution on $M(p_t) = \langle p_t \rangle$ measured by NA49 at 17.3 GeV; η scale (bin-size) dependence of three quantities measured by CERES: multiplicity in the angular acceptance, Φ_{p_t} and Σ_{p_t}.

A second measurement at the SPS was carried out by CERES. The results are shown in the last three panels of Fig. 2 [24]. A significant fluctuation excess was observed within a rapidity acceptance centered at the CM. That result is also notable as the first measurement of the scale or bin-size dependence of fluctuations (on η). Fig. 2 (second panel) shows multiplicity as a function of η scale, the third panel shows Φ_{p_t} as a function of η scale, and the fourth panel shows Σ_{p_t}. The data in the third panel permit partial reconstruction of the p_t angular correlations which produce $\langle p_t \rangle$ fluctuations at the SPS, an important SPS result.

In [24] it was argued that the similarity between the second and third panels implies that Φ_{p_t} is "proportional to" multiplicity, apparently a design defect of that measure, whereas $\sigma^2_{p_t,dynamical} \sim 2\sigma_{\hat{p}_t}\Phi_{p_t}/\bar{n}$ supposedly eliminates the offending factor $\bar{n}$. In fact, $\bar{n}$ and Φ_{p_t} are running integrals on scale of one- and two-particle momentum space and correctly reflect the structure of those spaces. $\sigma^2_{p_t,dynamical}$, the ratio of two running integrals, is therefore a *running average* of the underlying two-particle correlation (autocorrelation) which therefore presents a distorted picture of p_t angular correlations and suppresses localized p_t structure such as minijets.

After an initial null result [17], measurements by PHENIX provided the first indication of nonzero $\langle p_t \rangle$ fluctuations at RHIC [3]. Extensive measurements of several aspects of $\langle p_t \rangle$ fluctuations have subsequently been carried out by the STAR collaboration [2, 4, 5, 6]. Fig. 3 (first panel) presents a STAR measurement of the frequency distribution on $\sqrt{n}(\langle p_t \rangle - \hat{p}_t)/\sigma_{\hat{p}_t}$ (histogram) for Au-Au collisions at 130 GeV compared to a central-limit reference in the form of a gamma distribution (narrower curve) [2]. The variance excess is obvious for this measurement in the full STAR angular acceptance. The second panel shows the difference between data and reference in the first panel relative to the statistical error $\sqrt{N}$. The large statistical significance of the variance excess is indicated by deviations of up to *20 standard deviations* in each histogram bin. That STAR result suggested that unexpected phenomena might be present in RHIC collisions and initiated an era of precision differential measurements of p_t fluctuations and correlations.

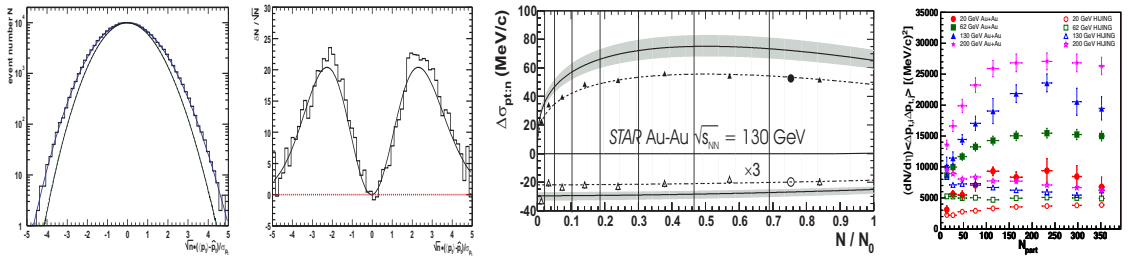

Figure 3: Frequency histogram on $\sqrt{n}(\langle p_t\rangle - \hat{p}_t)/\sigma_{\hat{p}_t}$ for 130 GeV central Au-Au collisions measured by STAR; corresponding difference between data and statistical reference in the first panel in units of the statistical error; the centrality dependence of $\Delta\sigma_{p_t:n} \approx \Phi_{p_t}$ for 130 GeV Au-Au collisions as in the first panel; comparable centrality dependence of $n_{ch}\langle \delta p_t \cdot \delta p_t\rangle$ for several energies measured by STAR.

The third panel shows the variation of difference factor $\Delta\sigma_{p_t:n} \sim \Phi_{p_t}$ with centrality, measured by particle multiplicity N relative to reference N_0 (for $b = 0$, central collisions). $\Delta\sigma_{p_t:n}$, defined by $\Delta\sigma^2_{p_t:n} \equiv 2\sigma_{\hat{p}_t}\Delta\sigma_{p_t:n}$ [2], facilitates comparison with Φ_{p_t} [18]. The centrality dependence is smooth, inconsistent with discontinuities expected by some to signal traversal of the QGP phase boundary. Measurements of $\bar{n}\langle \delta p_t \cdot \delta p_t\rangle$ (fourth panel) show similar behavior for several collision energies [5].

Those results demonstrated that large-amplitude $\langle p_t\rangle$ fluctuations are present in RHIC data and the fluctuation excess is smoothly varying with centrality, but the physical mechanisms responsible are not apparent. By studying the *scale dependence* of $\langle p_t\rangle$ fluctuations we can learn much more about their physical origins.

5. $\langle p_t\rangle$ fluctuation scale dependence and inversion

To answer the question "what phenomena produce $\langle p_t\rangle$ fluctuations" we define the relation between fluctuations and correlations. Fig. 4 (first panel) shows $\Delta\sigma^2_{p_t:n}(\delta\eta,\delta\phi)$—the p_t variance excess distributed on angular scales $(\delta\eta,\delta\phi)$. A fluctuation measurement at the full STAR TPC acceptance (Fig. 3, first panel) corresponds to the single point at the apex (upper endpoint) of the distribution on scale. Other points on the surface correspond to divisions of the acceptance into successively smaller bins (or detectors with smaller angular acceptances). The surface is structured and contains information on underlying p_t correlations, but the meaning is still not clear.

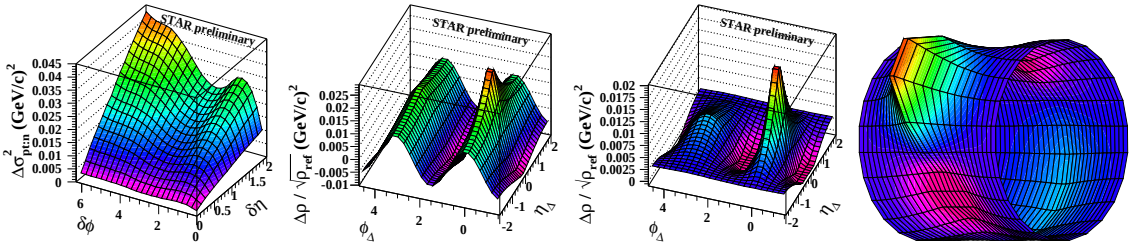

Figure 4: $\langle p_t\rangle$ fluctuation scale dependence on (η,ϕ) for 200 GeV mid-central Au-Au collisions measured by STAR; corresponding p_t angular autocorrelation obtained by inversion; the same autocorrelation after subtracting the elliptic flow contribution; the same data plotted in cylinder format.

Fluctuations in bins of a given size or scale are determined by two-particle correlations with characteristic lengths less than or equal to the bin scale. By measuring fluctuation magnitudes as a function of bin size one can recover some details of the underlying two-particle correlation structure—those aspects which depend on the *separation* of pairs of points, not on their absolute positions. The relation between fluctuations and correlations is given by the integral equation [15]

$$\Delta\sigma^2_{p_t:n}(m\,\varepsilon_\eta, n\,\varepsilon_\phi) = 4\sum_{k,l=1}^{m,n} \varepsilon_\eta\,\varepsilon_\phi \quad K_{mn;kl}\,\frac{\Delta\rho(p_t:n;k\,\varepsilon_\eta, l\,\varepsilon_\phi)}{\sqrt{\rho_{ref}(n;k\,\varepsilon_\eta, l\,\varepsilon_\phi)}}, \tag{5.1}$$

with kernel $K_{mn;kl} \equiv (m-k+1/2)/m \cdot (n-l+1/2)/n$ representing the 2D macrobin system. $\Delta\sigma^2_{p_t:n}(\delta\eta,\delta\phi)$ is a variance excess, and $\Delta\rho(p_t:n;)/\sqrt{\rho_{ref}(n)}$ is a normalized covariance density. That equation can be solved (inverted numerically) to obtain the p_t angular autocorrelation.

In Fig. 4 (second panel) we show the angular autocorrelation on difference axes $(\eta_\Delta,\phi_\Delta)$ (e.g., $\eta_\Delta = \eta_1 - \eta_2$) obtained by inverting the fluctuation scale dependence in the first panel. There are two major features: a sinusoid corresponding to "elliptic flow" and nonsinusoidal structure called "nonflow" in conventional flow terminology. This is the first observation of flow as a p_t correlation or velocity structure [4]. We can precisely remove the sinusoid, leaving the structure in the third panel which is dominated by minijet correlations, especially a same-side positive peak (jet cone) [4]. In the fourth panel we plot the same angular autocorrelation on $(\eta_\Delta,\phi_\Delta)$ in a cylinder format.

From the example in Fig. 4 we see that inversion of p_t fluctuation scale dependence to an autocorrelation provides direct physical interpretation of p_t fluctuation mechanisms. Parton fragment distributions (minijets) are visualized as event-wise temperature/velocity structures on (η,ϕ). A comprehensive picture of parton scattering, dissipation and fragmentation in heavy ion collisions is thereby established. In effect, we have determined the structure of the $\beta(\eta,\phi)$ temperature/velocity distribution on the prehadronic medium as promised. Fluctuation inversion is a Rosetta stone for fluctuation measurements, relating fluctuations to number and p_t angular autocorrelations. The newly-revealed structure of minijet p_t correlations in A-A collisions is further explored in Secs. 7 and 8.

6. Comparison: p_t angular autocorrelations by inversion and by pair counting

We have shown that p_t angular autocorrelations can be obtained from fluctuation inversion. They can also be obtained directly by pair counting [15]. In precision comparison tests the agreement between pair counting and inversion is excellent. The computation time for the former is $O(n^2)$, whereas for the latter it is $O(n)$. Thus, fluctuation inversion, especially for heavy ion collisions with very large data volumes, is the preferred route to p_t angular autocorrelations, offering a typical time saving of $10\times$ for minimum-bias RHIC Au-Au data at 200 GeV.

In Fig. 5 we show angular autocorrelations from fluctuation inversion (left panels) and pair counting (right panels). The left panels compare 200 GeV Au-Au peripheral collisions from RHIC data [4] and the Hijing Monte Carlo [20]. There are qualitative similarities but strong quantitative disagreements, even for peripheral collisions. The first and second panels are autocorrelations from 80-90% central Au-Au RHIC collisions and corresponding Hijing data respectively. The third and fourth panels are autocorrelations from 200 GeV p-p NSD minimum-bias and $n_{ch} \geq 18$ collisions

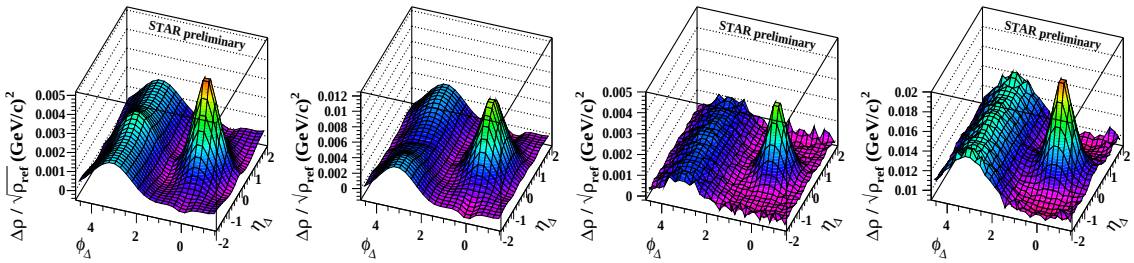

Figure 5: Left panels: p_t angular autocorrelations by fluctuation inversion from peripheral 200 GeV Au-Au collisions respectively for data and Hijing; Right panels: angular autocorrelations by pair counting from minimum-bias (NSD) 200 GeV p-p collisions and from collisions with $n_{ch} \geq 18$.

respectively. Those results represent the first determination of p_t angular autocorrelations in p-p and Au-Au collisions.

Angular autocorrelations either from fluctuation inversion or from pair counting provide precise results in peripheral A-A and p-p collisions. Small multiplicities present no problem for optimized fluctuation measures, as shown in Fig. 5. The analysis flexibility of properly designed measures coupled with well-defined centralities for all A-A collisions (including 90-100% centrality) [19] insure precise comparisons between A-A and p-p collisions and access to rapidly-evolving collision dynamics in mid-peripheral A-A collisions.

7. Model fits to Au-Au data

We established that p_t angular autocorrelations reveal underlying physical phenomena (minijets and elliptic flow). We now characterize Au-Au p_t autocorrelations quantitatively by fitting them with a model function, first subtracting sinusoid $\cos(2\phi_\Delta)$ (independent of pseudorapidity) associated with elliptic flow. A simple three-peak model describes the resulting data.

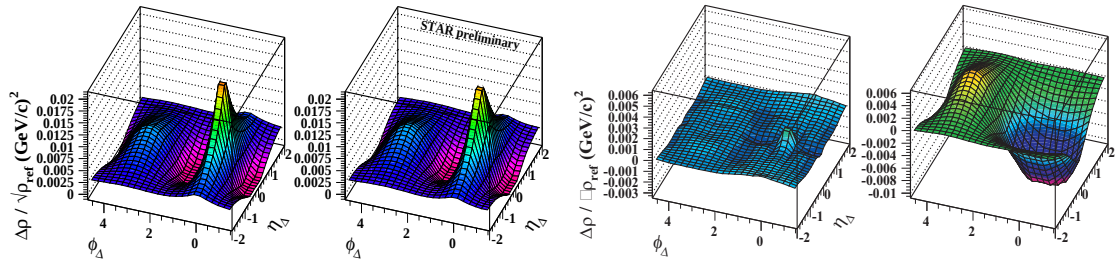

Figure 6: p_t angular autocorrelation for mid-central 200 GeV Au-Au collisions; a model fit; the fit residuals; the data autocorrelation (first panel) with the positive same-side model peak subtracted.

In fig. 6 (first panel) we show the p_t angular autocorrelation for 20-30% central 200 GeV Au-Au collisions with the flow sinusoid subtracted. The three-component model function (second panel) includes a same-side ($\phi_\Delta < \pi/2$) positive peak, a same-side negative peak and an away-side ($\phi_\Delta > \pi/2$) positive peak [4]. The model describes the data very well, as shown in the third panel. The vertical scale for the residuals is $3\times$ the first two panels, and the residuals are at the percent level.

A unique feature of these data is the negative regions on either side of the same-side postitive peak. Such structure has never been observed in angular correlations associated with jets. The

fourth panel shows the first panel (data) minus the same-side positive model peak. The resulting same-side negative peak is very different in shape from the positive peak—there is negligible systematic coupling in the fit procedure. That new feature of A-A collisions suggests an interesting interpretation presented in Sec. 9.

8. Data *vs* Hijing Monte Carlo

What does pQCD theory predict for p_t fluctuations and correlations? Applying the same techniques to Monte Carlo data we compare pQCD to RHIC data. In Fig. 7 (left panels, respectively) we compare results from 20-30% central 200 GeV Au-Au data (flow sinusoid subtracted) [4] with corresponding Hijing quench-on data [20]. Hijing does not predict η broadening of the same-side (SS) peak or the negative structure adjacent to the SS peak.

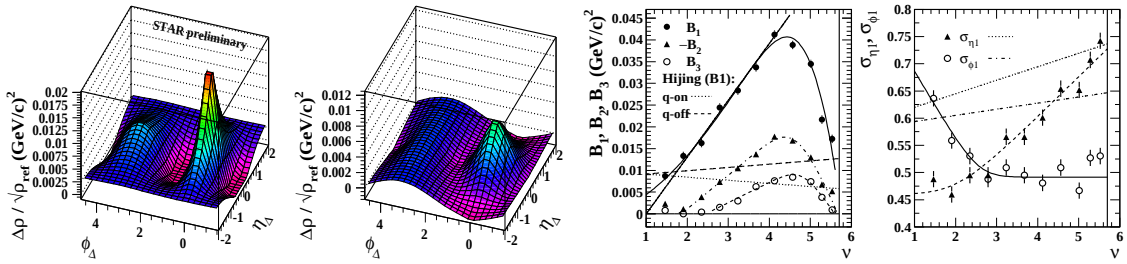

Figure 7: Left panels: a comparison of p_t angular autocorrelations from mid-central 200 GeV Au-Au data and corresponding quench-on Hijing; Right panels: the centrality dependence of the fit parameters from the three-peak model function.

The centrality dependence of peak amplitudes and widths is shown in Fig. 7 (right panels). Centrality is measured by path length ν, estimating the mean number of N-N collisions per participant pair [19]. The SS peak amplitude for RHIC Au-Au collisions in the third panel (solid dots) increases to more than $10\times$ the p-p amplitude before falling toward zero for the most central collisions. The SS negative peak ($-B_2$) first rises above zero at $\nu \sim 2$ and thereafter follows a pattern similar to the positive peak. In the fourth panel the positive SS azimuth width falls from p-p to central Au-Au, while the width on η increases sharply. Hijing trends represented by the straight dashed and dotted lines [20] are very different. Hijing quench-on (dotted line) predicts a decrease of the positive SS peak amplitude with centrality, whereas we observe a dramatic increase in the data. Quench-off Hijing (dashed line – transparent A-A collisions) predicts a modest 10% increase from peripheral to central collisions. The Hijing width trends in the fourth panel are also very different from data, especially the azimuth width.

To the extent that Hijing represents pQCD in A-A collisions the RHIC data in Fig. 7 are remarkably different from pQCD, albeit understandable in more general terms. Aside from the issue of jet quenching the disagreement between the solid data curve in the third panel and the dashed *quench-off* Hijing line represents a major problem for QCD theory. The measured minijet yield from heavy ion collisions with an *opaque central region* (e.g., disappearance of the away-side jet) is *four times larger* than a pQCD prediction for *transparent nuclei* (quench-off Hijing).

9. Recoil response of the QCD medium

In Fig. 8 we provide a possible interpretation of the negative structure in the p_t angular autocorrelations. In the first panel we repeat the angular distribution of the 200 GeV Au-Au p_t autocorrelation components *complementary to* the same-side positive peak. In the second panel we repeat the centrality dependence of the three peak amplitudes. We interpret the negative same-side peak in terms of red shifts and blue shifts of the local parent p_t spectrum and recoil of the medium.

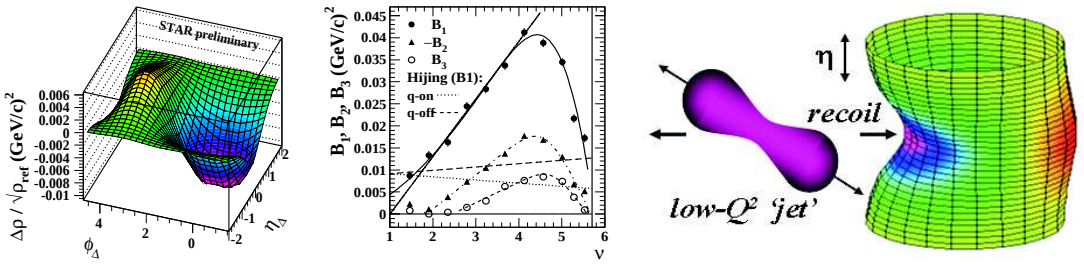

Figure 8: p_t angular autocorrelation from 200 GeV mid-central Au-Au collisions with elliptic flow and the postitive same-side model peak subtracted; centrality dependence of model peak amplitudes; illustration of parton scattering and fragmentation including data from the first panel replotted in cylinder format.

The p_t angular autocorrelation is a covariance distribution. A negative value for a given $(\eta_\Delta, \phi_\Delta)$ means that p_t sums in pairs of bins with that angular separation typically fluctuate in opposite directions (positive or negative deviation relative to the ensemble mean). A positive covariance means bins fluctuate in the same direction. From data in Fig. 4 we observe that in a region near the location of a minijet (positive covariance near the angular origin) p_t samples tend to be less than the ensemble average. In terms of spectrum shapes those local p_t spectra tend to be *red-shifted* relative to the ensemble mean, whereas local spectra nearest the minijet center tend to be blue-shifted relative to the mean.

"Blue shift" implies that parton fragmentation is described as hadron production from a source moving toward the observer, which is literally correct. "Red shift" implies that detected hadrons are apparently emitted from a source moving *away from* the observer relative to the average radial motion of the bulk medium. A spectrum red shift can therefore be interpreted as a consequence of *local recoil* of the bulk medium which has stopped the ingoing parton partner of the outgoing observed parton (positive same-side peak). Given that interpretation the centrality dependence is notable. The recoil amplitude ($-B_2$) in the second panel deviates from zero only above $\nu = 2$. There is no recoil until the average participant interacts with at least two projectile nucleons.

The last panel sketches the complete recoil picture. The typical minimum-bias outgoing parton (energy scale $Q \sim 4$ GeV) fragments to two hadrons (inferred from e^+-e^- fragmentation studies [23]). It's ingoing partner is stopped by the medium which absorbs the parton momentum as a recoil. The recoiling medium then emits or fragments to outgoing hadrons from a local spectrum red-shifted to lower p_t due to the ingoing recoil momentum. The cylinder (real data) illustrates the recoil distribution. The details of parton fragmentation and stopping in A-A collisions, including recoil response of the QCD medium suggested in the last panel, are accessed for the first time with p_t angular autocorrelations. The initial promise of p_t autocorrelations—the local velocity structure of the hadron source on (η, ϕ)—is thus realized.

10. Energy dependence of $\langle p_t \rangle$ fluctuations/correlations and low-Q^2 partons

Given the close connection between parton scattering and $\langle p_t \rangle$ fluctuations at RHIC the collision-energy dependence of $\langle p_t \rangle$ fluctuations could reveal previously inaccessible parton dynamics at lower (e.g., SPS) collision energies. In Fig. 9 (first panel) we show the centrality dependence of $\langle p_t \rangle$ fluctuations for four RHIC energies [6] and a summary (crosshatched region) of SPS fluctuation measurements at 12.6 and 17.3 GeV [24], all in the STAR TPC acceptance (the CERES measurements are extrapolated). In the second panel the pseudorapidity scale (bin size) dependence of fluctuations at full azimuth acceptance is shown for central collisions at six energies. Extrapolation of CERES data for the first panel is illustrated by the dashed lines at the bottom of the second.

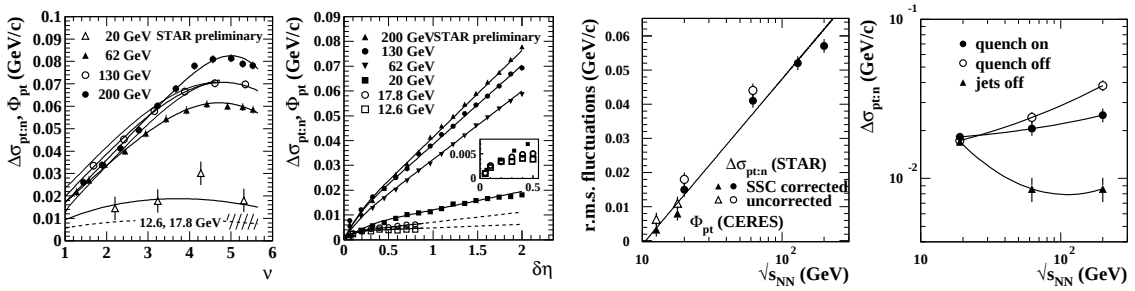

Figure 9: Centrality, pseudorapidity scale and energy dependence of $\langle p_t \rangle$ fluctuations for Au-Au collisions in the STAR acceptance; energy dependence for the Hijing Monte Carlo.

Φ_{p_t} was used for the CERES fluctuation measurements [24]. To good approximation $\Delta\sigma_{p_t:n} \simeq \Phi_{p_t}$ and both are *per particle* fluctuation measures which test linear superposition. For either measure we observe a dramatic increase in $\langle p_t \rangle$ fluctuations from SPS to RHIC energies. The centrality dependence in the first panel suggests that fluctuations in p-p and peripheral A-A collisions saturate at and above 60 GeV, whereas there is monotonic increase for the more central collisions. The scale dependence in the second panel illustrates how measurements with different detector acceptances are related. Measurements over common scale intervals should agree.

At the higher RHIC energies we have demonstrated that $\langle p_t \rangle$ fluctuations are dominated by fragments from low-Q^2 parton collisions. The energy dependence of $\Delta\sigma_{p_t:n}$ or Φ_{p_t} is shown in the third panel of Fig. 9, plotted *vs* $\sqrt{s_{NN}}$ [6]. We observe that $\langle p_t \rangle$ fluctuations in central collisions vary almost linearly as $\log\{\sqrt{s_{NN}}/10 \text{ GeV}\}$ (solid line in that panel), suggesting a threshold for *observable* transverse parton scattering and fragmentation near 10 GeV. In the fourth panel we encounter very different behavior for the Hijing Monte Carlo. The main difference is the strong contribution from low-p_t correlations representing longitudinal ('string') fragmentation in central Hijing collisions (all the correlations in "jets off" Hijing) which do not survive in central Au-Au collisions at RHIC [25]. Ironically, Hijing represents the QCD medium inconsistently, modeling high-p_t 'jet quenching' in the medium but not elimination of back-to-back longitudinal fragment correlations at low p_t.

Fluctuation measurements based on $\Sigma_{p_t} \simeq \sqrt{\Delta\sigma^2_{p_t:n}/(\bar{n}_{ch}\,\hat{p}_t^2)}$ [24] appear to contradict the strong energy dependence of $\langle p_t \rangle$ fluctuations, implying instead negligible energy dependence of $\langle p_t \rangle$ fluctuations from SPS to RHIC with a nearly constant value of 0.01 (1%) [24]. That conclu-

sion begs the question what are $\langle p_t \rangle$ fluctuations and how should they be measured? As noted, Σ_{p_t} is based on the assumption that each collision is thermalized with event-wise temperature T, that $\sigma^2_{p_t,dynamical} \sim \Delta\sigma^2_{p_t:n}/\bar{n}$ estimates temperature fluctuations as variance σ^2_T, and that the event-ensemble-average $p_t = \hat{p}_t$ estimates the ensemble mean T_0. If those assumptions were valid Σ_{p_t} would indeed estimate σ_T/T_0, with the implication that temperature fluctuations are independent of collision energy.

However, we observe that nuclear collisions at RHIC are dominated by *local* velocity structure from hard parton scattering. Events are not globally thermalized according to the assumptions used to support Σ_{p_t}. That measure averages the local p_t correlation structure dominating RHIC collisions over the entire detector acceptance, resulting in apparent *reduction* of correlations with increasing A-A centrality (as $1/N_{participant}$) and consequent insensitivity to hard scattering.

In our analysis we make no assumptions about thermalization. We study separately the changes in p_t production (T) and in the *correlation structure* of produced p_t (δT) *prior to hadronization*. We find that RHIC collisions are highly structured at kinetic decoupling, but differ qualitatively from a p-p superposition hypothesis. Our observations imply that equilibration or thermalization in heavy ion collisions is a quantitative issue requiring detailed measurements.

11. Summary

We have reviewed several p_t fluctuation measures and discussed their accuracy and interpretability. We described the relation between p_t fluctuations and event-wise variations in p_t spectrum shape over the angular space (η,ϕ). We made an analogy between p_t fluctuation measurements and measurements of the cosmic microwave background. First measurements at RHIC revealed that $\langle p_t \rangle$ fluctuations at 130 GeV are large, suggesting the need for and practicality of more differential methods. We then presented the integral equation which connects fluctuation scale dependence and angular autocorrelations. Results of fluctuation inversion have led to unambiguous interpretation of $\langle p_t \rangle$ fluctuations at RHIC.

p_t angular autocorrelations from Au-Au minimum-bias data reveal minijet correlations and elliptic flow. The minijet structure changes rapidly with collision centrality. We observe for the first time a large negative same-side peak under the positive minijet peak. The negative peak can be interpreted as recoil of the medium in response to stopping the in-going parton. Observation of recoil is possible only with p_t correlations. The Hijing Monte Carlo, representing pQCD with minijets as the dominant p_t correlation mechanism, is dramatically different from data. The increase of p_t fluctuations and correlations from SPS to RHIC is large. The $\ln(\sqrt{s}/10\ \mathrm{GeV})$ energy dependence is consistent with QCD expectations. That result also suggests that minijets also play a significant role at SPS energies.

This work was supported in part by the Office of Science of the U.S. DoE under grant DE-FG03-97ER41020.

References

[1] J. C. Collins and M. Perry, Phys. Rev. Lett. **34**, 1353 (1975);
B. Freedman and L. McLerran, Phys. Rev. D **17**, 1109 (1978);

G. Baym and S. A. Chin, Phys. Lett. B **62**, 241 (1976);
N. Cabibbo and G. Parisi, Phys. Lett. B **59**, 67 (1975).

[2] J. Adams *et al.* (STAR Collaboration), Phys. Rev. C **71**, 064906 (2005).

[3] S. S. Adler *et al.* (PHENIX Collaboration), Phys. Rev. Lett. **93**, 092301 (2004).

[4] J. Adams *et al.* (STAR Collaboration), J. Phys. G **32**, L37 (2006).

[5] J. Adams *et al.* (STAR Collaboration), Phys. Rev. C **72**, 044902 (2005).

[6] J. Adams *et al.* (STAR Collaboration), nucl-ex/0605021.

[7] k. Kajantie, P. V. Landshoff and J. Lindfors, Phys. Rev. Lett. **59**, 2527 (1987).

[8] A. H. Mueller, Nucl. Phys. B **572**, 227 (2000).

[9] G. C. Nayak, A. Dumitru, L. D. McLerran and W. Greiner, Nucl. Phys. A **687**, 457 (2001).

[10] J. Adams *et al.* (STAR Collaboration), Phys. Rev. D **74**, 032006 (2006).

[11] J. Adams *et al.* (STAR Collaboration), nucl-ex/0408012.

[12] C. L. Bennett *et al.* (WMAP Collaboration), AP Suppl. **148**, 1 (2003). http://map.gsfc.nasa.gov/

[13] R. J. Porter and T. A. Trainor (STAR Collaboration), Acta Phys. Polon. B **36**, 353 (2005).

[14] T. A. Trainor (STAR Collaboration), Proceedings of the International Symposium on Multiparticle Dynamics (ISMD 2005), Kromêříž, CR, August 9-15, 2005, Published in AIP Conf. Proc. **828**, 238 (2006).

[15] T. A. Trainor, R. J. Porter and D. J. Prindle, J. Phys. G: Nucl. Part. Phys. **31**, 809 (2005).

[16] S. A. Voloshin, V. Koch and H. G. Ritter, Phys. Rev. C **60**, 024901 (1999).

[17] K. Adcox *et al.* (PHENIX Collaboration), Phys. Rev. C **66**, 024901 (2002).

[18] M. Gazdzicki and S. Mrowczynski, Z. Phys. C **54** (1992) 127.

[19] T. A. Trainor and D. J. Prindle, hep-ph/0411217.

[20] Q. J. Liu, D. J. Prindle and T. A. Trainor, Phys. Lett. B **632**, 197 (2006).

[21] K. Pearson, Phil. Trans. Royal Soc. **187**, 253 (1896).

[22] T. A. Trainor, hep-ph/0001148

[23] T. A. Trainor and D. T. Kettler, Phys. Rev. D **74**, 034012 (2006).

[24] D. Adamova *et al.* (CERES Collaboration), Nucl. Phys. A **727**, 97 (2003).

[25] J. Adams *et al.* (STAR Collaboration), Phys. Rev. C **73**, 064907 (2006).

[26] H. Appelshauser *et al.* (NA49 Collaboration), Phys. Lett. B **459**, 679 (1999).

[27] T. Anticic *et al.* (NA49 Collaboration), Phys. Rev. C **70**, 034902 (2004).